Acta Cryst. (1990). B46, 703–712

Five-Dimensional Structure Analysis of Decagonal $Al_{65}Cu_{20}Co_{15}$

BY W. STEURER

Institut für Kristallographie und Mineralogie der Universität, Theresienstraße 41, *D*-8000 *München* 2, *Federal Republic of Germany*

AND K. H. KUO

Beijing Laboratory of Electron Microscopy, Chinese Academy of Sciences, PO Box 2724, 100080 *Beijing, People's Republic of China*

(*Received* 25 *April* 1990; *accepted* 20 *June* 1990)

Abstract

A single-crystal X-ray structure analysis of decagonal $Al_{65}Cu_{20}Co_{15}$ has been performed using the *n*-dimensional approach. Five-dimensional space group $P10_5/mmc$, $a_i^* = 0{\cdot}2656\ (2)$, $a_5^* = 0{\cdot}24107\ (3)$ Å^{-1}, $d_i = 3{\cdot}368\ (1)$, $d_5 = 4{\cdot}1481\ (3)$ Å, $\alpha_{ij} = 60$, $\alpha_{i5} = 90°$ ($i, j = 1,..,4$), volume of the five-dimensional unit cell $\Omega = 298{\cdot}2$ Å^5, $M_r = 39{\cdot}08$, $F(00000) = 15{\cdot}0$, $D_x = 4{\cdot}4$ Mg m^{-3}, $\mu = 12{\cdot}0$ mm^{-1}, Mo $K\alpha$, $\lambda = 0{\cdot}71069$ Å, $wR = 0{\cdot}098$ for 259 independent reflections with $I > 2\sigma(I)$ and 11 variables. The structure was solved by Patterson analysis and subsequent least-squares refinement, both in the five-dimensional description. There are three atoms in the asymmetric unit. Five-dimensional Fourier and difference Fourier syntheses show the pentagonal shape and chemical structure of the atoms parallel to the internal space. The three-dimensional decagonal structure is built up of periodically stacked sandwiches which consist of two planar quasiperiodic layers related by the tenfold screw axis. Characteristic large motifs of the crystalline $Al_{13}Fe_4$ structure type are found in a new arrangement in the quasiperiodic layers. The appearance of pentagonal channels which are partly empty or occupied statistically is noteworthy.

Introduction

Since the detection of quasicrystals six years ago hundreds of studies have been published laying the physical and crystallographic foundations of this new type of ordered matter. Most of the investigations have focused on three-dimensional quasiperiodic icosahedral phases, with fewer papers dedicated to the decagonal crystals which are quasiperiodic in two dimensions and periodic in the third. Initially, much theoretical work was concerned with the two-dimensional Penrose tiling which was assumed to be typical of a quasiperiodic layer. Henley (1986) discussed sphere packings and local environments of lattices of that type, and Levine & Steinhardt (1986) and Socolar & Steinhardt (1986) dealt with the definition and structure of two-dimensional quasicrystals as well as with possible unit-cell (thick and thin rhombi) configurations and local isomorphism classes. Jarič (1986) described fundamental diffraction characteristics, and Janssen (1986) introduced the *n*-dimensional approach for the description of quasicrystals. Kumar, Sahoo & Athithan (1986) treated the characterization and decoration of two-dimensional Penrose lattices. Pavlovitch & Klèman (1987) and Ishihara & Yamamoto (1988) studied the structural properties of general Penrose tilings applying the *n*-dimensional approach. Of course, this list of important papers is far from being complete.

Most of the experimental work on decagonal phases has been carried out on the systems Al–Mn and Al–Fe. Because of the lack of appropriate single crystals of these metastable quasicrystalline phases, powder diffraction or spectroscopic (*e.g.* EXAFS and NMR) techniques have been applied in nearly all quantitative investigations. The first single-crystal X-ray structure analysis on decagonal Al–Mn is described in Steurer & Mayer (1989) and Steurer (1989, 1990*b*). A short overview of the experimental work on decagonal Al–Mn may be found in Steurer (1989) and a detailed review on quasicrystal structure analysis is given in Steurer (1990*a*).

Detection of the decagonal phase in the system Al–Cu–Co provided the first example of a stable two-dimensional quasicrystal (He, Zhang, Wu & Kuo, 1988). Single crystals with decaprism morphology (μm and mm size) have since been grown by slow cooling from the melt (Kuo, 1988, 1989). The quality of these stable decagonal quasicrystals is high as indicated by selected-area electron diffraction, convergent-beam electron diffraction and X-ray diffraction patterns showing sharp Bragg reflections (He, Wu, Meng & Kuo, 1990). It can even be

0108-7681/90/060703-10$03.00

improved by adding a few percent of silicon as demonstrated for the Al–Mn–(Si) system. The Al–Cu–Co system is the only one which has decagonal quasicrystals with several possible translation periodicities along the tenfold axis: approximate values of 4, 8, 12 and 16 Å have been observed (He, Wu & Kuo, 1988), corresponding to two-, four-, six- and eight-layer stackings.

Almost all decagonal phases are closely related to crystalline phases with similar composition. These crystalline phases, as has been demonstrated by Zhang & Kuo (1990), may be interpreted as Penrose tiling approximants, at least in terms of the metrics. Consequently, the metrics of decagonal $Al_{65}Cu_{20}Co_{15}$ show a close resemblance to those of η-$Al_{13}Co_4$ (Hudd & Taylor, 1962), which has the $Al_{13}Fe_4$- (or $FeAl_3$-) type (Black, 1955*a*,*b*) structure. The monoclinic angle, $\beta = 107{\cdot}9\,(1)^\circ$, of the η-phase is very close to the value of 108° found for the tenfold symmetry of the decagonal phase. Its *b*-lattice parameter [$b = 8{\cdot}122\,(1)$ Å] is about twice the translation period $d_5 = 4{\cdot}1481\,(3)$ Å. On the one hand, the significant difference between $b = 8{\cdot}122\,(1)$ and $2d_5 = 8{\cdot}2962\,(6)$ Å (if the diffuse scattering leading to a doubling of d_5 is considered) is a simple proof that our crystal cannot be a decagonally twinned crystalline η-phase. On the other hand, it indicates a less-dense packing of the quasiperiodic layers than for the crystalline layers.

Transmission electron microscopy studies by Zhang & Urban (1989) provided the first evidence of the existence of extended planar defects and dislocations (mainly with the Burgers vector parallel to the tenfold screw axis) in this decagonal quasicrystal.

The aim of the present study is to give quantitative structural information about the decagonal phase using X-ray single-crystal techniques and to elucidate the structural relationships with the crystalline η-phase. By analogy with the regular three-dimensional structure analyses, however, only a kind of idealized average structure can result from the techniques applied. The condensation of the experimental Bragg peaks with finite full-width at half maximum (FWHM) to points on the quasiperiodic lattice nodes and the neglect of diffuse scattering imply an infinite quasicrystal built up of strictly ordered averaged atoms.

Higher-dimensional structure analysis

Why do we use and what is the meaning of a 'five-dimensional structure analysis'? The problem which we are confronted with when we want to solve the structure of decagonal $Al_{65}Cu_{20}Co_{15}$ is to transform the experimental information (intensities on the nodes of a quasiperiodic reciprocal lattice) into structural knowledge: in other words to determine what kind of atoms occupy which sites on a quasiperiodic direct lattice. The mathematical connection between the reciprocal and the direct-space information is given by the Fourier transform. Using intensities for Fourier coefficients the Patterson function (weighted vector diagram) results. With known structure factors (amplitudes and phases) electron density maps of the quasicrystal structure can be obtained. For a regular three-dimensional structure analysis the characterization of a finite (relatively small) unit cell facilitates the whole procedure for which numerous powerful techniques have been developed. In the case of aperiodic structures, however, it is not possible to define a finite three-dimensional unit cell either in direct or in reciprocal space.

An elegant way out of this dilemma, the *n*-dimensional approach, was first formulated by de Wolff (1974) for one-dimensional incommensurately modulated structures. It has been further developed by Janner & Janssen (1980*a*,*b*), de Wolff, Janssen & Janner (1981), Janssen (1986) and others, and may be employed in all cases of aperiodic structures which give diffraction patterns with sharp Bragg spots: the observed diffraction pattern is considered to be the projection of an *n*-dimensional periodic reciprocal lattice on the real three-dimensional world. For mathematical reasons, the three-dimensional aperiodic structure can then be found at the intersection of the *n*-dimensional periodic supercrystal with the real world. The dimension *n* necessary for the embedding is determined by the number *n* of rationally independent reciprocal basis vectors needed to index the diffraction pattern with integer numbers (quasilattice of rank *n*).

Because of the *n*-dimensional periodicity it is possible to define a simple *n*-dimensional unit cell and apply the conventional tools of crystallography, such as Fourier and Patterson syntheses, isomorphous substitution and contrast variation, in an extended form. In this way the structures of some quasicrystalline phases have been solved: icosahedral Al–Mn–Si by six-dimensional Patterson analysis (Gratias, Cahn & Mozer, 1988) and structure refinement (Cahn, Gratias & Mozer, 1988) as well as by isomorphous substitution (Janot, de Boissieu, Dubois & Pannetier, 1989); icosahedral Al–Cu–Li by contrast variation and subsequent six-dimensional refinement (de Boissieu, Janot, Dubois, Pannetier, Audier & Dubost, 1990) as well as by refining a six-dimensional structure model derived from a three-dimensional decorated Penrose tiling (van Smaalen, de Boer & Shen, 1990); decagonal Al–Mn by five-dimensional Patterson analysis (Steurer, 1989) and subsequent five-dimensional least-squares refinement (Steurer, 1990*b*).

These and other *n*-dimensional structure analyses have shown that the experimentally simple Patterson

method may be applied very successfully in *n*-dimensional crystallography (Steurer, 1987, 1990*a*), since the number of atoms in the *n*-dimensional unit cell of quasicrystals is generally very small and the resulting *n*-dimensional Patterson maps only exhibit a few maxima. Consequently, the atomic coordinates can be derived in a straightforward manner and may serve as starting parameters, together with arbitrary values for the other atomic parameters, in a subsequent least-squares structure refinement. By analogy with regular three-dimensional structure refinements, the positional parameters in the starting set have to be given to within a few tenths of an Å since they determine the phases of the structure factors. The shape parameters, given by a harmonic or anharmonic temperature factor in the three-dimensional case and, for example, by a pentagonal density function parallel to $\mathbf{V}_\parallel$ for a Penrose quasilattice, result more or less automatically from appropriate arbitrary starting values.

The goal of this type of structure refinement is to obtain a physically reasonable parameterization of the structure and derive the *phases* of the structure factors. The *n*-dimensional structure refinement is merely one necessary intermediate step in the course of the determination of the correct phases (signs), as it is in a regular three-dimensional structure analysis. The fitting procedure gives the best possible set of phases which is necessary for an optimal representation of the crystal structure in electron density maps resulting from the Fourier syntheses.

Experimental

A decaprismatic crystal of decagonal $Al_{65}Cu_{20}Co_{15}$, with approximate dimensions 0·05 × 0·07 × 0·08 mm, was mounted on top of a glass capillary, with the tenfold axis nearly parallel to it. The preparation and morphology of the crystal have been described in detail by He, Wu, Meng & Kuo (1990). X-ray precession (Fig. 1*a*) photographs show sharp Bragg reflections indicating a large coherence length of quasicrystalline regions. Scans on the four-circle diffractometer, however, gave FWHM about twice as large as for regular crystals on this instrument. There seems to be no dependence of the FWHM on the internal component of the diffraction vector $|\mathbf{H}_\perp|$. If one compares, for instance, the strong reflections along the straight line indicated in Fig. 1(*a*) the FWHM appears to be equal in spite of very different values for $|\mathbf{H}_\perp|$. One observes, however, small shifts of high $|\mathbf{H}_\perp|$ reflections from this straight line indicating some anisotropic linear phason strain (Steinhardt, 1987). Layers of diffuse scattering between layers of sharp Bragg reflections appearing on the cone-axis photographs (Fig. 1*b*) may result from one-dimensional partial ordering of chainlike quasicrystalline domains leading to a twofold translation period along the tenfold axis. The diffuse scattering is distributed in a similar manner to decagonal Al–Mn, whereas the diffuse streaks in decagonal Al–Fe are parallel to the tenfold screw axis.

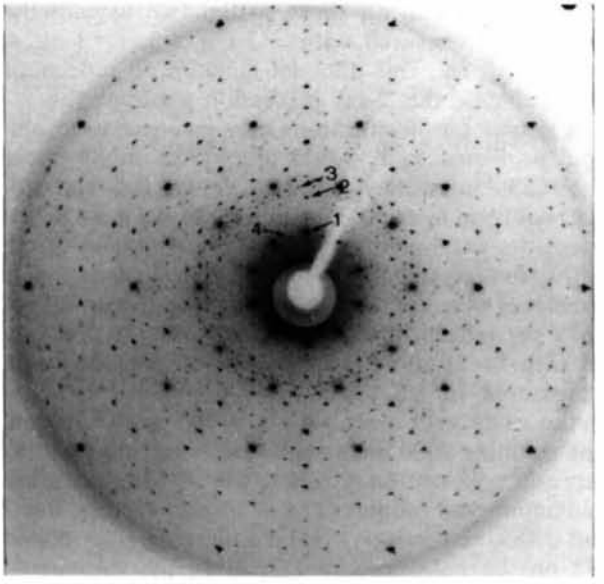

(*a*)

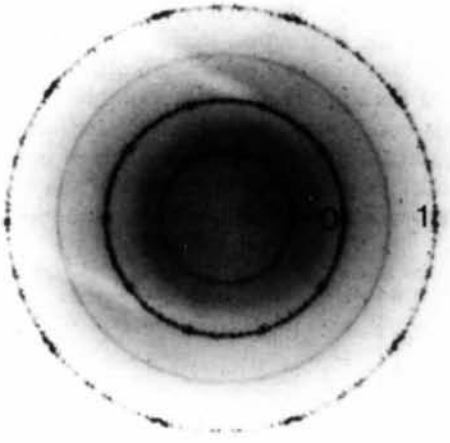

(*b*)

Fig. 1. (*a*) Zero-layer X-ray precession photograph of decagonal $Al_{65}Cu_{20}Co_{15}$. Some high and low $|\mathbf{H}_\perp|$ reflections are labeled: 1, (10000); 2, (00$\bar{1}$$\bar{1}$0); 3, (22$\bar{1}$20); 4, (2$\bar{1}$$\bar{1}$30); $|\mathbf{H}_\perp|$ is 0·27, 0·16, 1·09 and 0·92, respectively. Bragg spot 4 shows a significant shift from its ideal position on a straight line indicating some (rather small) anisotropic linear phason strain. (*b*) Cone-axis photograph with zero- and first-layer rings marked. Also visible are the diffuse layer rings causing a doubling of the d_5 lattice constant. On both photographs the more intense reflections are strongly overexposed to make weaker diffraction phenomena visible. [Mo $K\alpha$, focusing quartz monochromator, Rigaku RU 200 rotating-anode assembly, 0·3 × 0·3 mm fine focus, 60 kV, 90 mA, $\mu = 30°$, 148 h exposure time for (*a*) and 72 h for (*b*).]

Data collection

Enraf–Nonius CAD-4 four-circle diffractometer, Mo $K\alpha$ radiation, graphite monochromator. Lattice parameters refined from 24 reflections. $\omega/2\theta$ scans with $\omega = (1{\cdot}5 + 0{\cdot}35 \tan\theta)°$, extended 25% at each side for background determination. Out of the infinite number of possible reflections within $0 \le \theta \le 45°$ in a first run all those within two asymmetric units were measured with $-3 \le h_i \le 3$, $i = 1$ to 4, and $0 \le h_5 \le 8$. This data set includes all reflections observable on the X-ray precession photographs.

A denser set of reflections may give rise to resolution problems and would not yield many more observable intensities since it is known that the geometrical form factor g_k causes a rapid decrease of the intensities with increasing internal component of the diffraction vector (see Fig. 2). In this way, 2235 intensities were collected with a constant scan time of 120 s per reflection. The 260 reflections of this data set with $I > 2\sigma(I)$ and 32 additional reflections were remeasured in ten symmetrically equivalent asymmetric units with a scan time of 60 s per reflection. The resulting 2920 intensities were corrected for Lorentz and polarization effects as well as for absorption (maximum and minimum transmission factors: 0·607 and 0·483, respectively). After averaging ($R_i = 0{\cdot}062$) 292 unique reflections remained. In the subsequent structure refinements the 259 reflections with $I > 2\sigma(I)$ were included. The distribution of intensities as a function of the external and internal components of the diffraction vector is shown in Fig. 2 and illustrates possible truncation effects as a consequence of the limited data set available.

In this connection, the truncation effects parallel to the external and internal space are of comparable magnitude. For an ideal quasicrystal the intensities are densely distributed in the three-dimensional diffraction pattern. However, if we unfold the diffraction pattern into five-dimensional reciprocal space then the situation is analogous to that in the reciprocal lattice of a three-dimensional regular structure. Going to high indices parallel to the external space, the intensities fall off owing to the atomic form factor $f_k(\mathbf{H_E})$ (which has no influence on neutron diffraction) and the temperature factor $T_k(\mathbf{H_E})$. Parallel to the internal space the action of the geometrical form factor $g_k(\mathbf{H_I})$ and the phason factor $T_k(\mathbf{H_I})$ cause the diffraction peaks to fade away smoothly. Therefore, there is no danger in our case (Fig. 2) of *strong* disturbing ripples and spurious peaks in the Fourier or Patterson maps which would result from an abrupt truncation of a series of large Fourier coefficients.

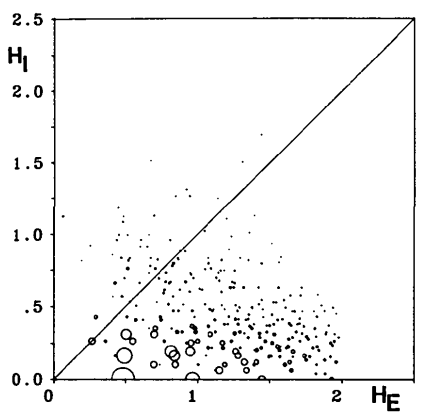

Fig. 2. Intensity statistics as a function of the internal *versus* the external component of the diffraction vector $\mathbf{H} = (\mathbf{H_E},\mathbf{H_I})$. The size of the circles is proportional to the respective structure amplitudes.

Symmetry and metrics

A detailed analysis of electron and X-ray diffraction patterns of decagonal Al–Cu–Co gives the Laue symmetry $10/mmm$ (D_{10h}), which together with the extinction rules, reduces the possible space groups to $P10_5mc$ and $P10_5/mmc$. From characteristic sections of the five-dimensional Patterson function (Fig. 3) it can easily be deduced that all atoms occupy special sites. The non-centrosymmetric space group can be rejected, therefore, at least in a first approximation.

All reciprocal lattice vectors of each quasiperiodic reciprocal lattice layer can be represented by linear combinations of five basis vectors pointing to the corners of a regular pentagon $\mathbf{a_i^*} = a_i^*(\cos 2\pi i/5, \sin 2\pi i/5, 0)$ with $i = 0,..,4$. The vector components refer to a Cartesian coordinate system with unit vectors $\mathbf{v_1}$, $\mathbf{v_2}$ and $\mathbf{v_3}$. Four of the five vectors are rationally independent. Perpendicular to the plane formed by this basis-vector set and parallel to the tenfold axis a further reciprocal basis vector $\mathbf{a_5^*} = a_5^*(0,0,1)$ is required. This set $\mathbf{M^*}$ of all reciprocal vectors $\mathbf{H_E} = \sum_{i=1}^{5} h_i \mathbf{a_i^*}$ in the external space $\mathbf{V_E}$ remains invariant under the action of the symmetry operators of the group D_{10h}. Since we have the same

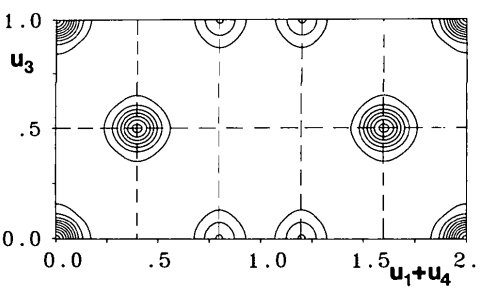

Fig. 3. Characteristic (10110) section of the five-dimensional Patterson function. All maxima of one five-dimensional unit cell are contained in this plane. All coordinates are given on the **V** basis.

situation as for decagonal Al–Mn (Steurer & Mayer, 1989; Steurer 1989) the same formalism holds for deriving the reflection indices, the five-dimensional symmetry and the metrics. Therefore, in the following only a summary of the results is given.

A basis for the representation of the lattice Σ^* in the five-dimensional configurational space **V** which is projected parallel to the internal space $\mathbf{V_I}$ onto $\mathbf{M}^*$ and is invariant under the action of the group D_{10h} can be written as $\mathbf{d_i}^* = (\mathbf{a_i}^*,0,c\mathbf{a_{3i}^*})$ with $i = 1,..,4$ and $\mathbf{d_5^*} = (0,\mathbf{a_5^*},0)$ (short **D** basis). c can be chosen arbitrarily without any consequence for physical space. If we refer the vectors $\mathbf{a_i}^*$ to a five-dimensional orthogonal coordinate system with unit vectors $\mathbf{v_i}$, $\mathbf{v_i}^*$ with $\mathbf{v_i v_j}^* = \delta_{ij}$ (short **V** basis) then we obtain the expression $\mathbf{d_i}^* = a_i^*(\cos 2\pi i/5, \sin 2\pi i/5, 0, c\cos 6\pi i/5, c\sin 6\pi i/5)$ with $i = 1,..,4$ and $\mathbf{d_5^*} = a_5^*(0,1,0)$. It should be kept in mind that the vectors $\mathbf{v_i}$, $\mathbf{v_i}^*$ with $i = 1,2,3$ belong to $\mathbf{V_E}$ and those with $i = 4,5$ to $\mathbf{V_I}$. The reciprocal lattice vector of the **D** basis has the form $\mathbf{H} = \sum_{i=1}^{5} h_i \mathbf{d_i}^*$. The basis of the direct five-dimensional lattice Σ is easily constructed by using the relationships $\mathbf{d_i}^* = a_i^* \sum_{j=1}^{5} U_{ji} \mathbf{v_j}^*$ and $\mathbf{d_i} = 1/a_i^* \times \sum_{j=1}^{5} u_{ij} \mathbf{v_j}$ with $(\mathbf{U_{ji}}) = [(\mathbf{u_{ij}})^{-1}]^T$ and we obtain $\mathbf{d_i} = 2/(5a_i^*)(\cos 2\pi i/5 - 1, \sin 2\pi i/5, 0, c\cos 6\pi i/5 - 1, c\sin 6\pi i/5)$ with $i = 1,..,4$, $\mathbf{d_5} = 1/a_5^*(0,0,1,0,0)$ and $\mathbf{d_i d_j}^* = \delta_{ij}$. The metric tensor $\mathbf{g}$ of the lattices Σ^* and Σ for the simple case $c = 1$ is given by

$$\mathbf{g} = \begin{pmatrix} A & C & C & C & 0 \\ C & A & C & C & 0 \\ C & C & A & C & 0 \\ C & C & C & A & 0 \\ 0 & 0 & 0 & 0 & B \end{pmatrix}$$

with $A = \mathbf{d_i^*}.\mathbf{d_i^*} = 2a_i^{*2}$, $B = \mathbf{d_5^*}.\mathbf{d_5^*} = a_5^{*2}$ and $C = \mathbf{d_i^*}.\mathbf{d_{j\neq i}^*} = -1/2a_i^{*2} = d_i^* d_j^* \cos 104{\cdot}5°$ for the reciprocal lattice Σ^* and $A = \mathbf{d_i}.\mathbf{d_i} = 4/(5a_i^{*2})$, $B = \mathbf{d_5}.\mathbf{d_5} = 1/a_5^{*2}$ and $C = \mathbf{d_i}.\mathbf{d_{j\neq i}} = 2/(5a_i^{*2}) = d_i d_j \cos 60°$ for the direct lattice Σ. Inserting the experimental values $a_i^* = 0{\cdot}2656\ (2)$ Å^{-1} $(i = 1,..,4)$ and $a_5^* = 0{\cdot}24107\ (3)$ Å^{-1} we obtain $d_i^* = 2^{1/2}a_i^* = 0{\cdot}3756\ (3)$ Å^{-1} $(i = 1,..,4)$ and $d_5^* = 0{\cdot}24807\ (3)$ Å^{-1} and $d_i = 2/(5^{1/2}a_i^*) = 3{\cdot}368\ (1)$ Å $(i = 1,..,4)$ and $d_5 = 4{\cdot}148\ (3)$ Å.

To describe the five-dimensional unit cell and to formulate the structure factor we use the **D** basis; for discussion of the characteristic features of the internal and external spaces with sections through the five-dimensional Fourier function the **V** basis is more appropriate.

Structure solution and refinement

The structure of decagonal $Al_{65}Cu_{20}Co_{15}$ was solved in a straightforward manner. The five-dimensional Patterson function (Fig. 3) is easy to interpret in a unique way and the coordinates for a model with two atoms in the asymmetric unit [atoms 1 and 2 of Fig. 5(*a*)] can be derived. These atoms occupy special positions on the body diagonal [11011] of the four-dimensional subcell as do four-dimensional atoms in the case of Penrose tiling (see, *e.g.*, Yamamoto & Ishihara, 1988). The site symmetry of these Wyckoff positions is *5mm*, *i.e.* *5m* [*cf.* Table 4.7 of Janssen (1988)] in the (00011) plane and *m* along [00100]. The shape of the five-dimensional atoms parallel to the internal subspace $\mathbf{V_I}$ has to be invariant applying that point symmetry. For general Penrose tilings this shape corresponds to irregular decagons [*cf.* Fig. 10 of Pavlovitch & Klèman (1987)]. Consequently, five-dimensional atoms of this kind in positions derived from the *n*-dimensional Patterson function, and with arbitrary atomic size paramater λ_k, have been used as the starting set for the five-dimensional least-squares refinements. The function minimized was $\chi^2 = \sum w_i(|F_{obs}(\mathbf{H})| - |F_{calc}(\mathbf{H})|)^2$, with weights $w_i = k/\sigma^2[F(\mathbf{H})]$ and $k = (N-1)/\chi^2_{min}$ (Prince, 1982). The reliability factors used were $R = (\sum||F_{obs}(\mathbf{H})| - |F_{calc}(\mathbf{H})||)/\sum|F_{obs}(\mathbf{H})|$ and $wR = \{\sum w_i[|F_{obs}(\mathbf{H})| - |F_{calc}(\mathbf{H})|]^2/\sum w_i|F_{obs}(\mathbf{H})|^2\}^{1/2}$. All sums are taken over $N = 259$ structure factors. The structure-factor formula applied in the refinements was

$$F(\mathbf{H}) = 1/\Omega_I \sum_k \exp(2\pi i \mathbf{H}.\mathbf{r_k}) f_k(\mathbf{H_E}) p_k T_k(\mathbf{H_E},\mathbf{H_I}) g_k(\mathbf{H_I})$$

where the diffraction vector $\mathbf{H} = (\mathbf{H_E}, \mathbf{H_I}) = \sum_i h_i \mathbf{d_i}^*$ $(i = 1,5)$, with $\mathbf{H_E} = h_1^E v_1^* + h_2^E v_2^* + h_3^E v_3^*$ and $\mathbf{H_I} = h_4^I v_4^* + h_5^I v_5^*$, which are the external and the internal components, respectively, of the diffraction vector. The positional vector $\mathbf{r_k}$ is given by $\sum_i x_i \mathbf{d_i}$ for atom k. The atomic scattering factor $f_k(\mathbf{H_E})$ depends only on the external component of the diffraction vector. The total site-occupancy factor p_k is $p_k^{Al} + p_k^{TM}$, where TM represents the transition metals Cu/Co. The temperature factor is given by

$$T_k(\mathbf{H_E},\mathbf{H_I}) = \exp\{-1/4[B_{11}^E(h_1^{E2} + h_2^{E2})a^{*2} + B_{33}^E h_3^{E2} + B^I(h_4^{I2} + h_5^{I2})a^{*2}]\}.$$

This expression contains the isotropic in-plane term B_{11}^E and the perpendicular component B_{33}^E, both in the external space, as well as one coefficient B^I in the internal space. The external temperature-factor components of the five-dimensional atoms have the same meaning as the temperature factor of a regular structure. The internal component, corresponding to smearing of the five-dimensional atom parallel to the internal space, leads to a higher frequency of intersections with physical space. Thereby, a number of interstitial sites become occupied at the cost of the regular ones. Consequently, displacive disorder may be described by the external part and substitutional disorder by the internal part of the temperature

factor. The geometrical form factor

$$g_k(\mathbf{H_I}) = (1/a^*)^2\Sigma_l \sin\theta_{l/l+1}\{A_l[\exp(iA_{l+1}\lambda_k) - 1] - A_{l+1}[\exp(iA_l\lambda_k) - 1]/[A_lA_{l+1}(A_l - A_{l+1})]\}$$

with $A_l = 2\pi\mathbf{H_I}.\mathbf{e_l}$ and $|\mathbf{e_l}| = 1/a_l^*$. $\Omega_\mathbf{I}$ is the area of the five-dimensional unit cell projected on $\mathbf{V_I}$.

The trial starting set for the five-dimensional least-squares refinement contained two atoms with irregular decagonal shape parallel to $\mathbf{V_I}$, which converged to regular pentagons during the course of the calculations. Therefore, the respective parameters have been reset to give this regular pentagonal shape and have not been refined further. The residual electron density in the difference Fourier maps indicated one additional atom which was included as atom 3 in the subsequent refinements. The internal temperature-factor coefficients, which refined to unphysical negative values or to values smaller than their standard deviations, were reset to zero and kept fixed during the remaining calculations. In addition, the thermal parameters of atoms 2 and 3 were constrained to common values. The five-dimensional atoms were assumed to be chemically homogenous parallel to $\mathbf{V_I}$ to reduce the number of variables. A possible chemical structure may be described by assigning Al and transition-metal atoms to different regions of the five-dimensional atoms corresponding to differently coordinated vertices [*cf.* Fig. 10 of Pavlovitch & Klèman (1987)]. With adequate resolution this chemical structure should become visible in difference Fourier syntheses as a deviation from a homogenous density distribution. The partial occupancy factors p_k^{Al} and p_k^{TM} have been constrained to give the chemical composition of the decagonal phase.

The refinements converged smoothly to $R = 0{\cdot}167$ and $wR = 0{\cdot}098$ for 259 reflections with $I > 2\sigma(I)$ and 11 variables. The quality of the least-squares fit is illustrated in an $F_{obs}(\mathbf{H})/F_{calc}(\mathbf{H})$ plot (Fig. 4). Small

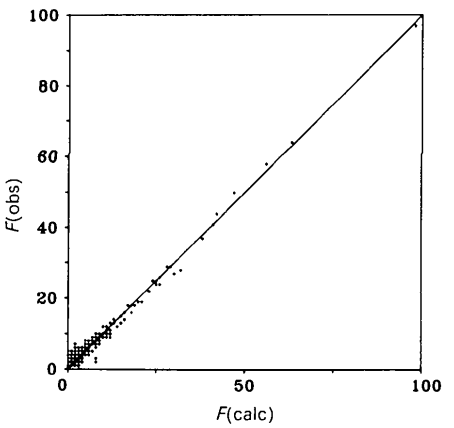

Fig. 4. $F_{obs}(\mathbf{H})/F_{calc}(\mathbf{H})$ plot for the final model.

significant deviations from the ideal distribution may result from deficiencies in the structure model since it neither accounts for the chemical structure of the five-dimensional atoms nor for the residual electron density appearing in the difference Fourier synthesis (Fig. 5). Another contribution may arise from systematic experimental errors during data collection. Despite these problems, the distribution in Fig. 4 indicates a highly reliable assignment of signs to the structure factors (in centrosymmetric structures, phases can only take on values of 0 and π, corresponding to the signs + and −). The slight changes in structure amplitudes which would bring all points in Fig. 4 onto the straight line would not entail a sign reversal, which would require the structure amplitudes to pass through zero.

The calculated density

The density of the refined structure model can be calculated in the following way: each section of a five-dimensional atom with the physical space gives an atom. The probability of such sections is proportional to the area $\Omega_k^\mathbf{I}$ of the internal component of the n-dimensional atom k. For the case $\Omega_k^\mathbf{I} = \Omega^\mathbf{I}$ (projection of the five-dimensional unit cell on $\mathbf{V_I}$) this probability becomes equal to one. Thus, the ratio $\Omega_k^\mathbf{I}/\Omega^\mathbf{I}$ gives the relative frequency of the three-dimensional atoms (vertices) generated from the

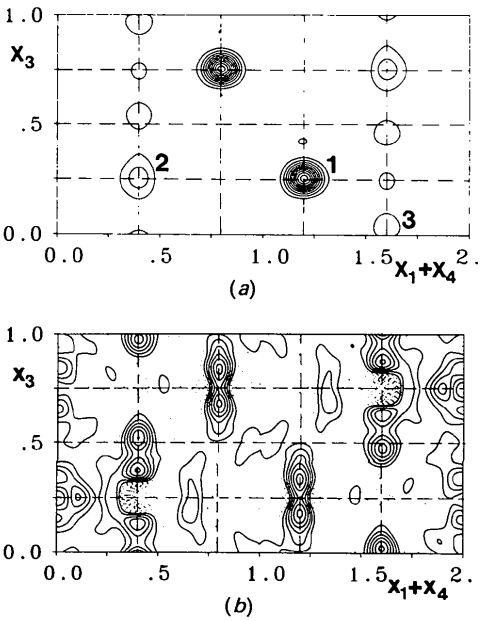

Fig. 5. (10110) sections of the five-dimensional (*a*) Fourier and (*b*) difference Fourier function calculated after the last refinement cycle using $F_{obs}(\mathbf{H})$ and $F_{obs}(\mathbf{H}) - F_{calc}(\mathbf{H})$, respectively, as Fourier coefficients. All coordinates are given on the V basis. The highest maximum in (*b*) amounts to about 4% of that in (*a*).

five-dimensional atom k. In our case the ratio $(\sum\Omega_k^{\mathbf{I}})/\Omega^{\mathbf{I}}$ amounts to 0·89. Consequently, each five-dimensional unit cell intersected by three-dimensional physical space generates 0·89 three-dimensional atoms on average. For numbers greater than one, atoms with too small a distance from each other might be generated. The number density $\rho_N = (\sum\Omega_k^{\mathbf{I}})/\Omega$ (Ω is the volume of the five-dimensional unit cell) gives the number of three-dimensional atoms (vertices) per unit volume. In our case $\rho_N =$ 0·070 vertices Å^{-3} corresponding to a mean atomic volume of 14·3 Å^3 compared with 15·6 Å^3 for crystalline $Al_{13}Co_4$. Knowing the number density, the density of the quasicrystal can be calculated as $\rho_c = M_r\rho_N/N_L$ (N_L corresponds to the Avogadro number). Inserting the experimental values we obtain $\rho_c =$ 4·4 Mg m^{-3} (since the experimental density of the decagonal phase is not yet known, the density of a fictitious mixture of the elements with the composition $Al_{65}Cu_{20}Co_{15}$ is given for comparison as $\rho =$ 4·8 Mg m^{-3}). The density of the η-phase, which can be written as $Al_{76.5}Co_{23.5}$, is $\rho = 3{\cdot}81$ (5) Mg m^{-3} (Hudd & Taylor, 1962).

Results and discussion

Table 1 lists the refined atomic parameters in terms of the five-dimensional description.* All refined atoms occupy special sites ($x_i = n/5$, $i = 1,..,4$) as is the case for the two-dimensional Penrose tiling. This confirms the assumption of Yamamoto & Ishihara (1988) that the layers making up decagonal structures consist of partial Penrose tilings. The external thermal parameters (which contain dynamic and static components) are similar to those of regular structures. The values of the internal temperature-factor components show that it is not necessary to account for phasons which would be described by a large internal temperature factor.

A more vivid impression of the structural characteristics than that obtained by a numerical description can be conveyed by special sections of the five-dimensional Fourier and difference Fourier functions. Thus, Fig. 5(*a*) shows a Fourier map of the (10110) plane containing all atoms in the five-dimensional unit cell. The maxima marked 1, 2 and 3, and their symmetry equivalents, correspond to the atoms included in the refinements. Some additional maxima appear on the difference Fourier map (Fig. 5*b*); the maximum peak heights are about 4% of that of atom 1 in the Fourier map. The peak distances to the next-nearest atoms are approximately 0·2–0·3 Å

Table 1. *Parameters of the five-dimensional atoms of decagonal* $Al_{65}Cu_{20}Co_{15}$ *with e.s.d.'s in parentheses*

The parameters listed are fractional atomic coordinates x_i (**D** basis), two external (B^E_{11}, B^E_{33}) and one internal (B^I) temperature-factor coefficient (Å^2), total site-occupancy factor p_k, partial Al-occupancy factor p_k^{Al} of that site, and the radial atomic size parameter λ_k as a fraction of $1/a_i$* (negative λ_k denotes opposite direction of $\lambda_k\mathbf{e}_i$).

Parameter	Atom 1	Atom 2	Atom 3
Site symmetry	*5mm*	*5mm*	*5m*
Multiplicity	2	2	4
x_1	$\frac{2}{5}$	$\frac{4}{5}$	$\frac{1}{5}$
x_2	$\frac{2}{5}$	$\frac{4}{5}$	$\frac{1}{5}$
x_3	$\frac{2}{5}$	$\frac{4}{5}$	$\frac{1}{5}$
x_4	$\frac{2}{5}$	$\frac{4}{5}$	$\frac{1}{5}$
x_5	$\frac{1}{4}$	$\frac{1}{4}$	0·04 (1)
B^E_{11}	1·22 (8)	1·8 (2)	1·8
B^E_{33}	0·34 (6)	2·2 (3)	2·2
B^I	0·00	0·00	0·00
p_k	1·00	0·86 (9)	0·25 (5)
p_k^{Al}	0·08	1·00	1·00
λ_k	−0·335 (2)	0·444 (5)	0·16 (2)

indicating a statistical substitutional disorder which is larger for atom 2 than for atom 1. In addition, the short distance (1·1 Å) between atoms 2 and 3 only permits an alternating occupation of these sites. Indeed, this is reflected in the reduced occupation probabilities of 0·86 (9) for atom 2 and 0·25 (5) for atom 3. Further disorder is indicated by the residual electron density along the [00100] direction. It should be noted that the related crystalline η-$Al_{13}Co_4$ structure also shows some substitutional disorder, which is indicated by three partially occupied Al sites (Hudd & Taylor, 1962).

Looking at the (00011) sections of the five-dimensional Fourier and difference Fourier function (Fig. 6), which characterize the internal space component of the five-dimensional atoms, the pentagonal shape of the atoms parallel to this plane is easily recognized. The deviations of the layer-line plot from the regular pentagonal form (drawn with the refined pentagonal-size parameter λ_k) result from the chemical structure as can be seen in the difference Fourier maps. The refined structure model contains five-dimensional chemically homogenous atoms and the deviations from this given homogeneity are represented by the difference Fourier plots. If one compares, for instance, the relative peak heights at the left-hand corner of the pentagons of atom 1 in Figs. 6(*a*) and 6(*b*) one finds that the model displays an electron density that is about 15% too high in the region corresponding to the fivefold vertex ${}^5_2J$ [see Fig. 8 of Pavlovitch & Klèman (1987)]. Consequently, it is Al atoms which primarily occupy these vertex positions in the three-dimensional quasi-periodic structure, whereas the other vertices are occupied by transition-metal atoms.

Similarly, one finds that the center of the five-dimensional atom 2, which consists completely of Al

* A list of structure factors has been deposited with the British Library Document Supply Centre as Supplementary Publication No. SUP 53320 (3 pp.). Copies may be obtained through The Technical Editor, International Union of Crystallography, 5 Abbey Square, Chester CH1 2HU, England.

according to our model, should contain about 20% less electron density. This can be explained by the alternating statistical occupation of the three-dimensional atoms generated from the centers (corresponding to the regular fivefold vertex ${}^5_5S$ in the three-dimensional structure) of the atoms 2 and 3, which is necessary because of the short distance (1·1 Å) between these atoms. The radially decreasing density of the atoms parallel to $\mathbf{V}_1$ reflects series-termination effects rather than a decreasing occupation probability.

Structure of the layers

What do the quasiperiodic layers which make up the structure of the decagonal phase look like? The planes at $x_3 = \frac{1}{4}$ and $\frac{3}{4}$ are symmetrically equivalent and related by a 36° rotation followed by a shift of $\frac{1}{2}$ parallel to [00100]. Fig. 7 shows real-space (11000) sections ($\sim 22 \times 22$ Å) of the five-dimensional Fourier function, in which the solid lines illustrate characteristic features. The (10010) sections are also shown in each case, to make the correspondence of three- and five-dimensional maxima clearer.

In Fig. 7(*a*) the highest maxima (corresponding to Cu/Co atoms) are connected so as to give a network of pentagons and thin rhombi. Each rhombus is decorated asymmetically with one weak Al peak. The pentagons (edge length about 4·7 Å) contain three or five weak maxima (Al), which are quite broad in some cases, indicative of displacive disorder. The (10010) section in the lower part of Fig. 7(*a*) links the real three-dimensional quasiperiodic and the five-dimensional periodic structure. One unit cell is marked as containing the atoms 1 and 2. The dashed line corresponds to the line at $x_3 = \frac{1}{4}$ in Fig. 5(*a*). One sees clearly that the center of atom 2 has a lower density than at its periphery. Another important feature is that the atoms 2 and 1 occur in pairs, connected by a low density, which indicates some substitutional disorder.

Fig. 7(*b*) shows differently connected maxima in order to point out the close resemblance of the structures of the quasiperiodic layer of decagonal $Al_{65}Cu_{20}Co_{15}$ with those of the $y = \frac{1}{4}$ layer of crystalline $Al_{13}Fe_4$ [*cf.* Fig. 4 of Black (1955*b*)]. The half unit cell of $Al_{13}Fe_4$ is marked with a dash-dotted line. Despite small shifts and a slightly different distribution of Al and transition-metal atoms this structure element appears to be the same in both phases. Because of their higher transition-metal content, however, some Al atoms occuring in the crystal-

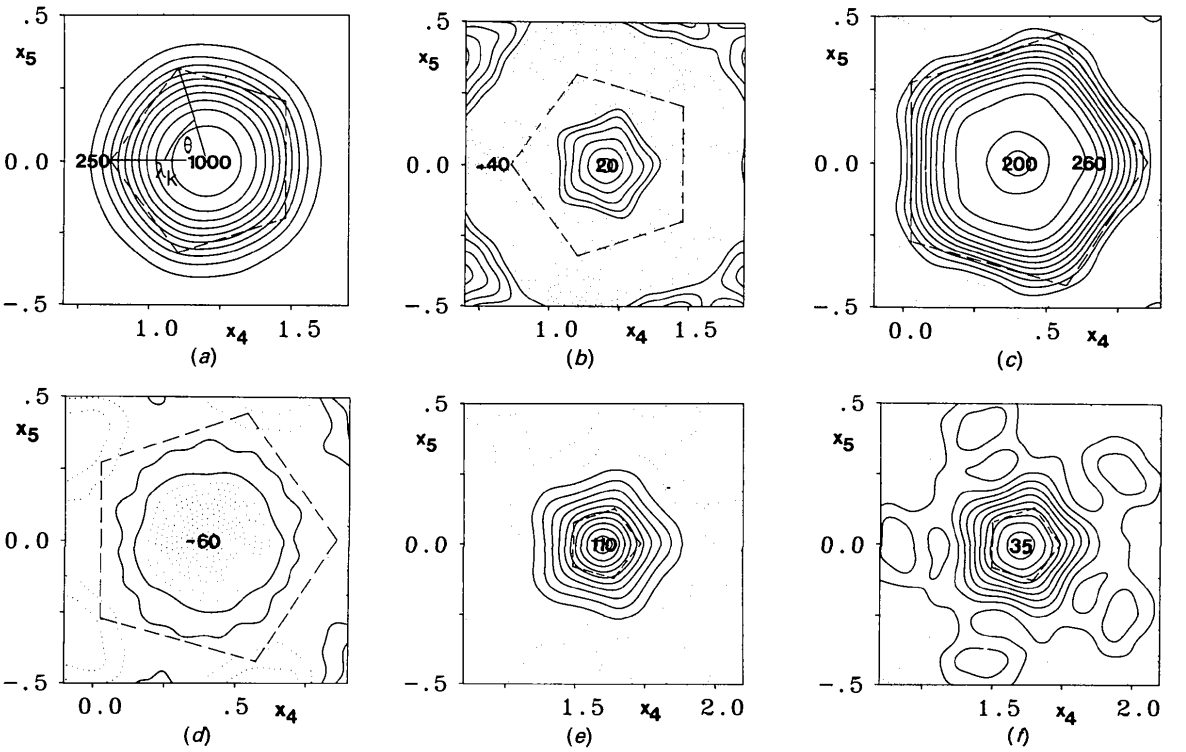

Fig. 6. (00011) sections (parallel to the internal space $\mathbf{V}_1$) of the five-dimensional Fourier and difference Fourier functions, respectively, of atom 1 in (*a*) and (*b*), atom 2 in (*c*) and (*d*) and atom 3 in (*e*) and (*f*). All coordinates are given on the V basis. Relative peak heights are given in arbitrary units. The dashed-line pentagons have been plotted according to the size parameter λ_k resulting from the refinements.

line phase have to be replaced by Cu/Co atoms. The pentagons of the network in Fig. 7(*b*) possess an edge length of 2·9 Å, smaller then those marked in Fig. 7(*a*) by a factor of $1/\tau$. Henley (1985) and Kumar, Sahoo & Athithan (1986) have already pointed out that the puckered layer of the $Al_{13}Fe_4$ structure may be considered to be a relaxed decorated two-dimensional Penrose tiling.

One finds alternating filled and empty pentagons in the quasiperiodic layer as well as in the crystalline one. But, in contrast to the crystalline case, the quasiperiodic layers are stacked in such a way as to form a set of pentagonal channels parallel to [00100] which are empty or occupied statistically, alternating with corner atoms. This is illustrated in Fig. 7(*c*) which shows the projection of the structure on (11000) [Fourier synthesis calculated with $F(h_1h_2h_3h_40)$ only]. Despite the disordered content of these channels their centers always remain empty. The (10010) section of the projected structure makes it clear that atom 3 is projected on the low-density center of atom 2 and sums to give a fully occupied atomic site.

Stacking of the layers

The three-dimensional decagonal structure results from stacking the quasiperiodic layers, rotated 36° in each case, one upon another. Because of the pentagonal rotation symmetry, only the stacking order *ABAB*... is possible. Therefore, decagonal Al–Cu–Co phases with larger periodiocities cannot result from simple stacking variations as in most polytypes. The three-dimensional coordination polyhedra are almost the same as those occurring in the $Al_{13}Fe_4$ structure [*cf.* Fig. 1 of Black (1955*b*)]. Consequently, the interatomic distances in the quasiperiodic and periodic crystal structures are quite similar.

What are the principal structural differences between the quasiperiodic and periodic phases? First, the formation of a set of pentagonal channels, formed by Cu/Co atoms and occupied in a more or less disordered way, may play a role. Secondly, the transition-metal subset forms a well ordered network in a similar way to the $y = 0$ layer in $Al_{13}Fe_4$ [*cf.* Fig. 3 of Black (1955*b*)]. However, in contrast to $Al_{13}Co_4$ or the isostructural $Al_{13}Fe_4$, which exhibit 'vacant regions and inefficient packing' (Black, 1955*b*), the quasiperiodic layers seem to be better accommodated by substituting part of Al and Co by Cu. Thirdly, these rearrangements allow the building up of the decagonal structure by stacking one type of layer alone. The two slightly different layers of the $Al_{13}Fe_4$ structure type with their 'misfit regions' and the 'Al_{14} in the flat layer (which) is not in contact with any atoms of that layer' (Black, 1955*b*) seem to be a poor compromise, which can only be overcome by the pentagonal long-range ordering of the quasiperiodic layers.

A comparison with the structure of decagonal $Al_{78}Mn_{22}$ (Steurer, 1990*b*) shows a striking similarity of the projected (down 10_5) structures. Qualitatively, this can also be deduced from the great similarity of the respective zero-layer X-ray or electron diffraction patterns. The only significant difference lies in the occupation of the tenfold clusters of pentagonal

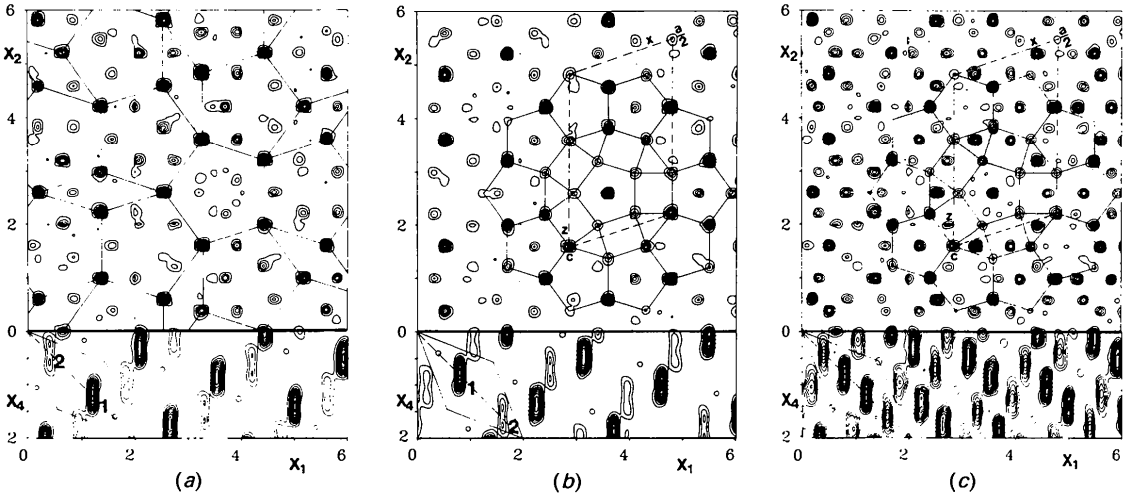

Fig. 7. Quasiperiodic (11000) sections (parallel to the external space V_E with a size of about 22 × 22 Å) of the five-dimensional Fourier function of decagonal $Al_{65}Cu_{20}Co_{15}$ at (*a*) $x_3 = \frac{1}{4}$ and (*b*) $x_3 = \frac{3}{4}$. Characteristic structure motifs are marked which can also be found in slightly distorted form in the $Al_{13}Fe_4$-type structures. The edge length of the large pentagons in (*a*) is 4·7 Å and of the small ones in (*b*) 2·9 Å. (*c*) The quasicrystal structure projected down the tenfold screw axis [calculated from reflections $F(h_1,h_2,h_3,h_4,0)$ only]. Additionally, the respective (10010) sections are shown to enable the correspondence between the five- and three-dimensional structures to be visualized. All coordinates are given on the V basis.

rings: in the present case these pentagons are filled alternately, whereas all of them are full in the case of decagonal Al–Mn. The main difference between the decagonal phases is the different layer-stacking sequence and the existence of two different layers in the asymmetric unit for the Al–Mn structure. However, both have in common the fact that their structural building elements are similar to those of crystalline $Al_{13}Fe_4$, and that there appear to be no Mackay icosahedra. The most characteristic structural elements are the pentagonal channels clustered in tenfold rings.

KHK is grateful to the Chinese National Natural Science Foundation for financial support and to Mr L. X. He for the growth of the single quasicrystal used in this study.

References

BLACK, P. J. (1955*a*). *Acta Cryst.* **8**, 43–48.
BLACK, P. J. (1955*b*). *Acta Cryst.* **8**, 175–182.
BOISSIEU, M. DE, JANOT, C., DUBOIS, J. M., PANNETIER, J., AUDIER, M. & DUBOST, B. (1990). *J. Phys. Condens. Matter.* Submitted.
CAHN, J. W., GRATIAS, D. & MOZER, B. (1988). *J. Phys. (Paris)*, **49**, 1225–1233.
GRATIAS, D., CAHN, J. W. & MOZER, B. (1988). *Phys. Rev. B*, **38**, 1643–1646.
HE, L. X., WU, Y. K. & KUO, K. H. (1988). *J. Mater. Sci. Lett.* **7**, 1284–1286.
HE, L. X., WU, Y. K., MENG, X. M. & KUO, K. H. (1990). *Philos. Mag. Lett.* **61**, 15–19.
HE, L. X., ZHANG, Z., WU, Y. K. & KUO, K. H. (1988). *Inst. Phys. Conf. Ser.* **93**, 501–502.
HENLEY, C. L. (1985). *J. Non-Cryst. Solids*, **75**, 91–96.
HENLEY, C. L. (1986). *Phys. Rev. B*, **34**, 797–816.
HUDD, R. C. & TAYLOR, W. H. (1962). *Acta Cryst.* **15**, 441–442.
ISHIHARA, K. N. & YAMAMOTO, A. (1988). *Acta Cryst.* A**44**, 508–516.
JANNER, A. & JANSSEN, T. (1980*a*). *Acta Cryst.* A**36**, 399–408.
JANNER, A. & JANSSEN, T. (1980*b*). *Acta Cryst.* A**36**, 408–415.
JANOT, C., DE BOISSIEU, M., DUBOIS, J. M. & PANNETIER, J. (1989). *J. Phys. Condens. Matter*, **1**, 1029–1048.
JANSSEN, T. (1986). *Acta Cryst.* A**42**, 261–271.
JANSSEN, T. (1988). *Phys. Rep.* **168**, 55–113.
JARIĆ, M. (1986). *Phys. Rev. B*, **34**, 4685–4698.
KUMAR, V., SAHOO, D. & ATHITHAN, G. (1986). *Phys. Rev. B*, **34**, 6924–6932.
KUO, K. H. (1988). *Proceedings of an International Workshop on the Application of Electron Microscopy to Materials Science, Gaungzhou, China*, edited by K. H. KUO, pp. 153–168. Trans Tech.
KUO, K. H. (1989). *Solid State Phenom.* **5**, 153–168.
LEVINE, D. & STEINHARDT, P. J. (1986). *Phys. Rev. B*, **34**, 596–616.
PAVLOVITCH, A. & KLÈMAN, M. (1987). *J. Phys. A*, **20**, 687–702.
PRINCE, E. (1982). *Mathematical Techniques in Crystallography and Materials Science.* New York: Springer-Verlag.
SMAALEN, S. VAN, DE BOER, J. L. & SHEN, Y. (1990). *Phys. Rev. B.* Submitted.
SOCOLAR, J. E. S. & STEINHARDT, P. J. (1986). *Phys. Rev. B*, **34**, 617–647.
STEINHARDT, P. J. (1987). *Mater. Sci. Forum*, **22–24**, 23–44.
STEURER, W. (1987). *Acta Cryst.* A**43**, 36–42.
STEURER, W. (1989). *Acta Cryst.* B**45**, 534–542.
STEURER, W. (1990*a*). *Z. Kristallogr.* **190**, 179–234.
STEURER, W. (1990*b*). *J. Phys. Condens. Matter.* Submitted.
STEURER, W. & MAYER, J. (1989). *Acta Cryst.* B**45**, 355–359.
WOLFF, P. M. DE (1974). *Acta Cryst.* A**30**, 777–785.
WOLFF, P. M. DE, JANSSEN, T. & JANNER, A. (1981). *Acta Cryst.* A**37**, 625–636.
YAMAMOTO, A. & ISHIHARA, K. N. (1988). *Acta Cryst.* A**44**, 707–714.
ZHANG, H. & KUO, K. H. (1990). Preprint.
ZHANG, Z. & URBAN, K. (1989). *Philos. Mag. Lett.* **60**, 97–102.

Acta Cryst. (1990). B**46**, 712–716

Structure of Hexaaquacobalt(II) Bromate

BY ANTHONY C. BLACKBURN, JUDITH C. GALLUCCI AND ROGER E. GERKIN*

Department of Chemistry, The Ohio State University, Columbus, Ohio 43210, *USA*

(*Received* 12 *February* 1990; *accepted* 20 *June* 1990)

Abstract

$[Co(H_2O)_6](BrO_3)_2$, $M_r = 422{\cdot}83$, cubic, $Pa\bar{3}$, $a = 10{\cdot}3505\ (7)$ Å, $V = 1108{\cdot}88\ (8)$ Å^3, $Z = 4$, $D_x = 2{\cdot}53$ g cm^{-3}, λ(Mo $K\bar{\alpha}$) $= 0{\cdot}71069$ Å, $\mu = 87{\cdot}31$ cm^{-1}, $F(000) = 820$, $T = 296$ K, $R = 0{\cdot}027$ for 365 unique reflections having $I > \sigma_I$. The single type of Co ion is coordinated by six water-molecule O atoms, each at an observed distance 2·095 (2) Å, in an array which is regular octahedral within the estimated standard deviations of the relevant angles. The single type of bromate ion has a Br—O bond length 1·653 (2) Å and O—Br—O bond angle 104·07 (9)°. The cobalt–oxygen complex manifested rigid-body behavior, but the bromate ion did not. The cobalt–oxygen distance corrected for rigid-body motion is 2·099 Å. Location and refinement of the two inequivalent H atoms permitted detailed analysis of the hydrogen bonding, which occurs principally between the oxygen octahedra and the bromate groups. This structure is isomorphic to that of hexaaquanickel(II) chlorate recently reported from this laboratory.

* Author for correspondence.

0108-7681/90/060712-05$03.00